Rheological and Thermomechanical Properties of Long-Chain-Branched Polyethylene Prepared by Slurry Polymerization with Metallocene Catalysts

Edward Kolodka,[1,*] Wen-Jun Wang,[1,†] Shiping Zhu,[1,2] Archie Hamielec[1]

[1]*Department of Chemical Engineering, McMaster University, 1280 Main Street West, Hamilton, Ontario, Canada L8S 4L7*
[2]*Department of Materials Science and Engineering, McMaster University, 1280 Main Street West, Hamilton, Ontario, Canada L8S 4L7*

Received 24 February 2003; accepted 13 September 2003

ABSTRACT: A series of polyethylene (PE) samples were prepared in a slurry polymerization with bis(cyclopentadienyl) zirconium dichloride (Cp_2ZrCl_2)/modified methylaluminoxane (MMAO) using a semibatch reactor. The samples had long-chain branch densities (LCBDs) of a 0.03–1.0 branch per 10,000 carbons and long-chain branch frequencies (LCBFs) up to a 0.22 branch per polymer molecule. The rheological and dynamic mechanical behaviors of these long-chain branched PE samples were evaluated. Increasing the LCBF significantly increased the η_0's and enhanced shear thinning. Long-chain branching (LCB) also influenced the loss modulus and storage modulus. Increasing the LCBF led to enhanced G' and G'' values at low shear rates and broader relaxation spectrums. The samples exhibited thermorheologically complex behavior. LCB also played a significant role in the dynamic mechanical behavior. Increasing the LCBF increased the stiffness of the polymer and enhanced the damping or energy dissipation. However, LCB had little influence on the crystalline structure of the PE. The α- and γ-relaxations showed little dependence on the LCBF.
 J Appl Polym Sci 92: 307–316, 2004

Key words: polyethylene (PE); long chain branching; characterization; rheology; mechanical property

INTRODUCTION

There has been much research focused on establishing the relationships between the molecular architecture and the processing/materials properties of polyolefins in recent years.[1–8] The influence of long-chain branching (LCB) on the viscoelastic/mechanical behavior of polymers can be remarkable.[9,10] The precise effects of LCB are not well understood, however, due to the difficulty of producing well-defined samples with a broad range of molecular attributes. There are many molecular properties which influence the physical characteristics of polymers including the molecular weight, molecular weight distribution (MWD), short-chain branching (SCB), LCB, branch length, and branch frequency distribution. These properties act in concert and separating individual influences has proven to be difficult.

Extremely low levels of LCB have been shown to have significant influence on the viscoelastic behavior of polyolefins. Carella et al.[4] observed significantly enhanced zero-shear viscosities (η_0) compared to linear polymers with similar molecular weights in star-branched hydrogenated polybutadienes (HPBs). It was demonstrated that the η_0 of star-branched HPBs varied exponentially with the arm molecular weight. Further studies by Jordan et al.[11] on asymmetric three-arm star HPBs determined that the length necessary for a branch to behave as a long-chain branch was $2M_e$. It has been shown that the M_e for PE is 1250. Yan et al.[12] observed significant enhancements in η_0, shear thinning and flow-activation energies in LCB polyethylene (PE) produced in a continuous stirred tank reactor (CSTR) using a constrained geometry catalyst (CGC).

Recent innovations in single-site-type catalysts allow the preparation of polymers with narrow MWDs.[13,14] Dow Chemical's CGC was used to synthesize long-chain branched PEs of various molecular weights and long-chain branch densities (LCBDs).[15,16] This catalyst, with its open configuration, produces LCB through the insertion of vinyl-terminated PE formed *in situ* through β-hydride elimination or chain transfer to the monomer. Recently, we reported a continuous solution polymerization of ethylene[15] and the shear-thinning properties of the resulting long-chain

Correspondence to: S. Zhu (zhuship@mcmaster.ca).
**Present address:* Department of Chemical Engineering, University of North Dakota, Grand Forks, ND 58202-8155.
†*Present address:* Nexwood Industries Inc, Brampton, Toronto, ON, Canada L6T 5R5.
Contract grant sponsor: Ministry of Education, Science and Technology of Ontario (MEST).

TABLE I
Molecular Properties of Long-chain-branched PE Samples Prepared by Semibatch Slurry Polymerization

Sample	$M_n \times 10^{-3}$ (g/mol)	$M_w \times 10^{-3}$ (g/mol)	M_w/M_n	LCBD[a]	LCBF[a]
1	115	280	2.44	0.25	0.16
2	60.6	154	2.54	0.33	0.12
3	46.2	108	2.34	0.10	0.03
4	38.9	95	2.44	0.73	0.22
5	46.4	122	2.63	0.65	0.21
6	74.1	197	2.66	0.30	0.15
7	66.7	160	2.40	0.35	0.17
8	54.1	152	2.81	0.21	0.07
9	29.3	63	2.15	1.00	0.20
10	27.8	57	2.05	0.86	0.17

Polymerization conditions: catalyst, Cp_2ZrCl_2; cocatalyst, MMAO (12 mol % of isobutylaluminoxane); solvent, toluene; solvent volume, 700 mL.
[a] Determined by ^{13}C-NMR.

branched PEs.[12] We also reported the preparation of long-chain branched PEs using a semibatch slurry process.[17] In this work, we report experimental data for the thermorheological and dynamic mechanical properties of long-chain branched PEs prepared by the slurry process.

EXPERIMENTAL

Materials, polymerization procedure, and GPC/^{13}C-NMR measurements

A series of long-chain branched PEs were produced in a slurry-phase semibatch reactor using zirconocene dichloride/modified methylaluminoxane (MMAO). The materials, polymerization procedure, GPC, and ^{13}C-NMR characterization were reported elsewhere.[17] The molecular properties of the samples are summarized in Table I.

The PE samples were blended with a 0.6 wt % Irganox 1010 antioxidant to prevent degradation. The antioxidant was dissolved in acetone and mixed with the polymer powder. The acetone was evaporated for 24 h in a fumehood and the polymer dried in a vacuum oven for 48 h at 80°C. The samples were then melt-pressed (20-mm diameter, 2-mm thickness) at 180°C and 2 MPa for 6 min, followed by rapid quenching.

Rheological measurements

The rheological measurements were conducted on a Stresstech HR parallel-plate rheometer in the dynamic mode with a gap of 1.5 mm. Samples were placed in the rheometer, heated to the measurement temperature, and allowed to equilibrate for 10 min. The parallel plates were then moved to a gap of 1.5 mm and the excess polymer was trimmed. Samples were measured in 10°C increments between the temperatures of 170–210°C under a nitrogen blanket to prevent degradation. Strain sweeps were performed prior to frequency sweeps to establish the linear region. A frequency range of 10^{-2} to 65 s^{-1} was investigated using a variable strain method. This method entails using the maximum strain that is within the linear region. The influence of the long-chain branched frequency (LCBF) on the storage modulus G' (ω), loss modulus G''; (ω), and complex viscosity η^*, as defined in eq. (1), were investigated:

$$\eta^* = \left[\left(\frac{G'}{\omega}\right)^2 + \left(\frac{G''}{\omega}\right)^2\right]^{\frac{1}{2}} \quad (1)$$

Mechanical measurement

The mechanical properties of the polymers were measured using a TA Instruments DMA 2980 dynamic mechanical analyzer. The storage modulus E', the loss modulus E'', and the loss tangent tan δ ($= E'/E''$) were measured between -140 and 130°C. A heating rate of 2°C/min and a displacement of 2 μm were employed. The thermal transitions were taken as the temperature of the maximum of E''. The measurements for all the samples were made at identical conditions and were repeated twice for a valid and reliable comparison of the results.

RESULTS AND DISCUSSION

Effect of LCBF on shear thinning

The LCB samples had very long relaxation times at low shear rates and it was not possible to obtain frequency-independent viscosities from which the Newtonian viscosities (η_0) could be inferred. An attempt at fitting the viscosity data using the Cross equation,[18] given by eq. (2), was made:

$$\eta^*(\omega) = \frac{\eta_0}{[1 + (\lambda\omega)^n]} \quad (2)$$

where the value of n was assumed to be independent of the temperature and the characteristic time, λ, to be inversely proportional to η_0. The value of λ was approximated as $365{,}000/\eta_0$. Unfortunately, solutions were not found for these samples. Figure 1 shows samples 2 and 8 fitted using eq. (2). The Cross equation gave a good approximation of the viscosity at high shear rates for both samples. At low shear rates, the equation still gave an adequate estimation for sample 8 (LCBF = 0.07) but performs poorly for sample 2 (LCBF = 0.22). The Cross equation failed at low shear rates for nonlinear polymers. Therefore, η_0 was approximated with the complex viscosity measured at

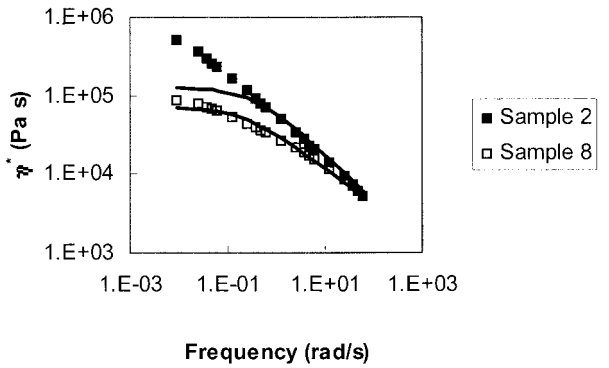

Figure 1 Dynamic viscosity at 190°C fit with the Cross equation.

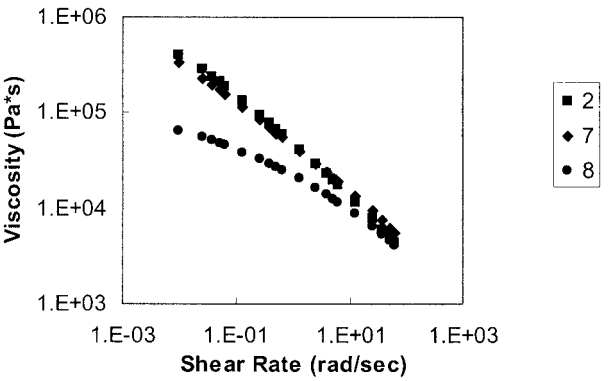

Figure 2 Dynamic viscosity of PE samples with M_w of approximately 155 kg/mol.

$\omega = 0.01\ s^{-1}$. To quantify the shear-thinning behavior, the power-law expression, given by eq. (3), was fitted to the viscosity data at high shear rates:

$$\eta = m\dot{\gamma}^{n-1} \tag{3}$$

where m is the consistency, and n, the power-law exponent which indicates the degree of non-Newtonian behavior.

The LCBF of slightly branched PE has been shown to have a major role in its rheological behavior. However, distinguishing the effects of LCB from the influences of the molecular weight and the polydispersity index is challenging. The η_0 of polymers above the critical entanglement length (M_C) is related to the M_w by eq. (4):

$$\eta_0 = KM_W^{3.4} \tag{4}$$

Consequently, doubling the M_w has the effect of increasing η_0 by an order of magnitude. Therefore, when comparing the rheological characteristics of polymers, it is essential that the M_w's be similar. To this end, the long-chain branched PEs were divided into three groups: Group 1 was composed of samples 2, 7, and 8 with M_w's of 154, 160, and 152 kmol/g, respectively. Group 2 compared samples 4 and 5 having M_w's of 95 and 122 kmol/g, while group 3 compared samples 9 and 10 with M_w's of 63 and 57 kg/mol. When the M_w's of the PE samples were similar, the LCBF had a significant influence on the dynamic viscosity. Figure 2 shows the dynamic viscosity of samples 2, 7, and 8 versus the frequency at 190°C.

The LCBF influenced the rheological responses: LCB significantly enhanced the low shear viscosity. By comparing samples 2 and 8 with LCBFs of 0.12 and 0.07, respectively, we observed a sevenfold increase in the low shear viscosity. It must be further emphasized that these samples had similar M_w's and that this enhancement was attributed solely to the effect of LCB. At higher shear rates, these samples all exhibited similar viscosities. This behavior was also observed in samples 9 and 10 as shown in Figure 3. These samples had similar M_w's, 63 and 57 kmol/g, but LCBFs of 0.20 and 0.17, respectively. Branching again enhanced the low shear viscosity while having little influence on the high shear viscosity.

The flow behavior in Figures 2 and 3 can readily be explained by observing the molecular architecture of the polymer samples. At low shear rates, the viscosity is dominated by the relaxation behavior of the branched polymer molecules. The long-chain branches can form entanglements with nearby polymer chains. These entanglements function as temporary physical crosslinks, significantly increasing the resistance to flow. An increase in the branch frequency increases the amount of entanglements, leading to enhanced low shear viscosities. At high shear rates, however, the viscosity is dominated by the flow of linear chains. The long-chain branches become aligned with the polymer backbones, breaking the temporary physical crosslinks. Consequently, samples with similar M_n's but different levels of LCB are expected to exhibit similar high shear viscosities. This behavior was indeed observed in Figures 2 and 3. At low shear

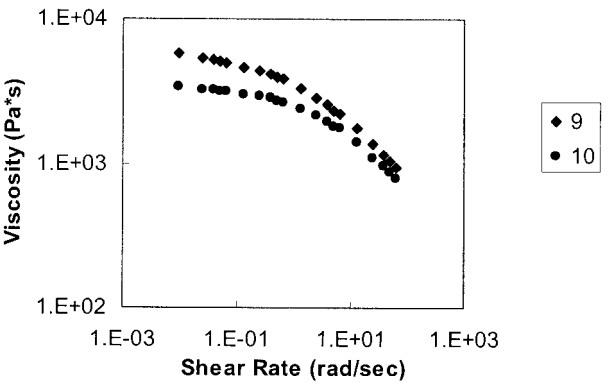

Figure 3 Dynamic viscosity of PE samples with M_w of approximately 60 kmol/g.

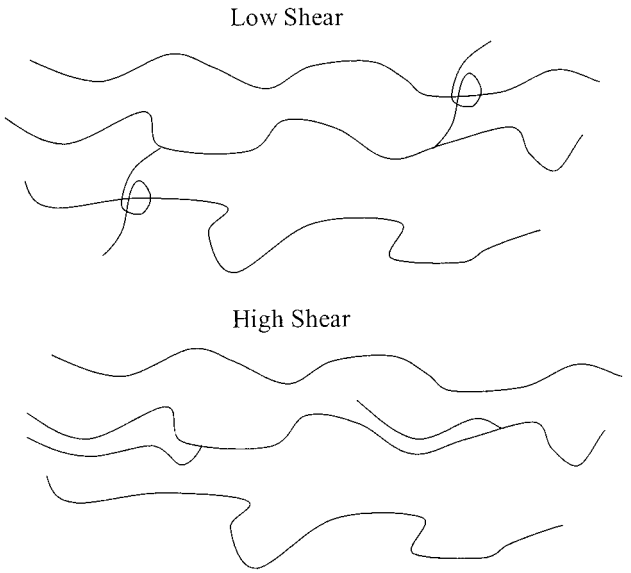

Figure 4 Schematic representation of LCB at high and low shear rates.

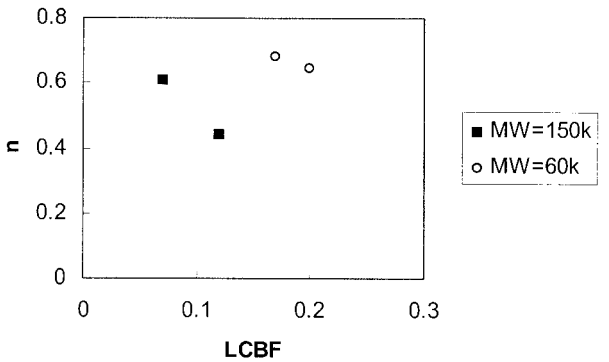

Figure 5 Influence of LCBF on the power-law exponent n.

rates, the viscosity of the polymer with higher levels of LCB exhibited significantly higher low shear viscosities. When the shear rate approached 100 s^{-1}, the viscosities almost overlapped.

The mechanism of the LCB effect is schematically illustrated in Figure 4. In both diagrams, there are three polymer chains with the middle molecule having two LCBs. At low shear rates, the branches entangle with nearby polymers, increasing the resistance to flow. At higher shear rates, the branches align with the polymer backbone, preventing entanglements.

A method of characterizing the magnitude of the shear-thinning behavior is to fit the high shear viscosity with the power-law expression given in eq. (3). The value of n indicates the degree of shear thinning, with a value of 1 signifying Newtonian behavior and lower values indicating increased shear thinning. The values obtained for n are given in Table II. Figure 5 shows the influence of LCBF on the power-law exponent for samples 2 and 8 (M_w's = 150 kmol/g) and samples 9 and 10 (M_w = 60 kmol/g).

When the M_w's of the samples were similar, an increase in the LCBF decreased the value of n, indicating an increase in the shear-thinning phenomenon. This is readily explained by the increase in entanglements afforded by the increase in LCBs. Another interesting effect was the influence of the M_w. Despite having lower LCBFs, samples 2 and 8 both had lower values of n. Furthermore, it was observed that the slope of a line connecting samples 2 and 8 was significantly steeper than was a line connecting samples 9 and 10. This indicated that an increase in the LCBF at elevated M_w's produced a greater effect on shear thinning than did a similar increase at lower M_w's.

The influence of branching on the shear-thinning phenomenon was also compared with the samples having different M_w's. The shear viscosity was normalized by dividing by η_0 and plotted versus the frequency. This technique eliminated the changes in η_0 caused by varying the M_w and focused on the shear-thinning phenomenon attributed to LCB. The smaller the ratio of η to η_0, the greater was the amount

TABLE II
Viscosity and Relation Properties of Long-chain-branched PE Samples

Sample	η_0[a] (Pa s)	n	α-Relaxation (°C)	β-Relaxation (°C)	γ-Relaxation (°C)
1	NA	NA	53.24	—	−117.15
2	4.06×10^5	0.437	52.19	—	−115.72
3	NA	NA	52.35	—	−115.69
4	7.86×10^4	0.518	52.51	—	−116.50
5	1.11×10^5	0.520	51.93	—	−115.43
6	7.14×10^5	0.442	NA	NA	NA
7	3.27×10^5	0.506	NA	NA	NA
8	6.46×10^4	0.606	51.46	—	−115.41
9	5.80×10^3	0.642	NA	NA	NA
10	3.43×10^3	0.679	49.13	—	−115.56

Polymerization conditions: catalyst, Cp_2ZrCl_2; cocatalyst, MMAO; solvent, toluene; solvent volume, 700 mL. NA: not available.

[a] Measured at 190°C.

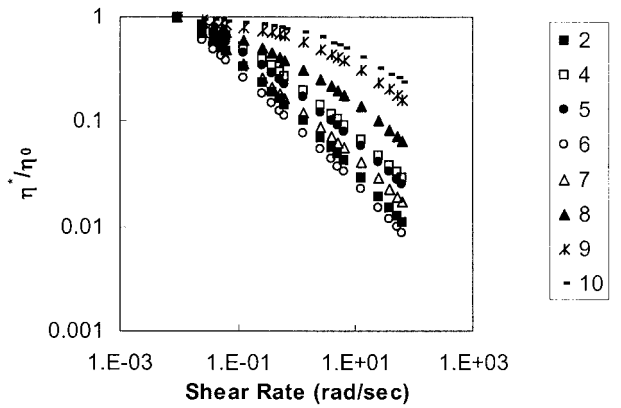

Figure 6 Normalized dynamic viscosity of the PE samples.

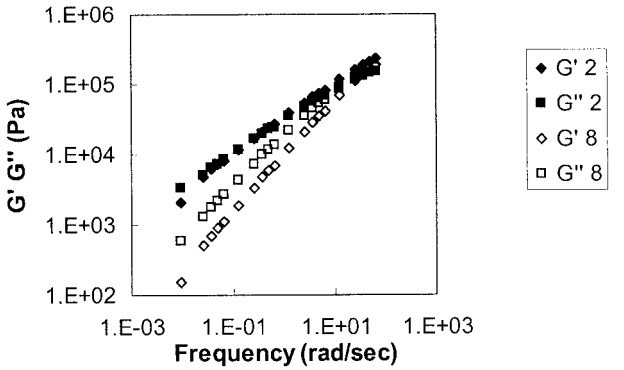

Figure 7 Influence of LCBF on G' and G'' for samples 2 and 8.

of shear thinning. Figure 6 shows the normalized viscosity responses of the long-chain-branched PEs produced in a slurry-phase semibatch reactor.

Another mechanism, separate from the LCBF, appeared to influence the shear viscosity. Samples with similar M_w's and different LCBFs behaved in an expected manner. Sample 2, with an M_w of 154 kmol/g and an LCBF of 0.12, exhibited significantly more shear thinning than that of sample 8, with an M_w of 152 kmol/g and an LCBF of 0.07. Sample 2 had a greater amount of LCBs and, consequently, more entanglements formed at low shear rates, increasing the shear-thinning phenomenon. However, when comparing sample 7, with an LCBF of 0.17 and an M_w of 160 kmol/g, with sample 10, with an LCBF of 0.17 and an M_w of 57 kmol/g, it was apparent that another mechanism occurred. Despite having similar LCBFs, these samples had significantly different flow behavior. Sample 7 showed considerable shear thinning, while sample 10 exhibited almost no shear thinning.

This behavior was attributed to the influence of the LCB length. LCB in homo-PE produced in a semibatch slurry reactor was thought to be due to the incorporation of vinyl-terminated macromonomers produced earlier in the reaction. The kinetics of formation of a macromonomer and a dead polymer chain were similar and they, therefore, had similar molecular weights. Consequently, polymers produced with high molecular weights had a high molecular weight macromonomer incorporated into their growing backbones as LCBs. These longer branches were involved in greater entanglements, leading to elevated low shear viscosities. Consequently, a polymer cannot simply be characterized by knowing the LCBF. Information about the branch length must also be known. This behavior was observed in sample 5 (LCBF = 0.21, M_w = 122 kmol/g) and sample 9 (LCBF = 0.20, M_w = 63 kmol/g). Despite having similar LCBFs, sample 5 exhibited significantly greater shear thinning.

Effect of LCBF on shear modulus and thermorheological complexity

The influence of the LCBF on the storage modulus (G') and the loss modulus (G'') was also studied. Figure 7 shows G' and G'' versus the frequency for samples 2 and 8. Despite having similar M_w's, samples 2 and 8 had different rheological responses. Sample 2, with an M_w of 154 kmol/g and an LCBF of 0.12, had enhanced values of G' and G'' at low shear rates compared to sample 8, with an M_w of 152 kmol/g and an LCBF of 0.07. However, at higher shear rates, the values of G' and G'' were similar for these samples. Sample 2 also had a broader relaxation spectrum evident by the more gradual increase of G'. These effects were attributed to the additional modes of relaxation at low shear rates due to branching. Unfortunately, it was not possible to determine the plateau modulus (G'_0), a characteristic viscoelastic parameter which could be used to determine the molecular weights between entanglements (M_e), for these samples. The loss modulus plateau was located at a shear rate outside the experimental shear range. Samples 9 and 10 behaved in a similar manner. Figure 8 shows G' and G'' versus the frequency.

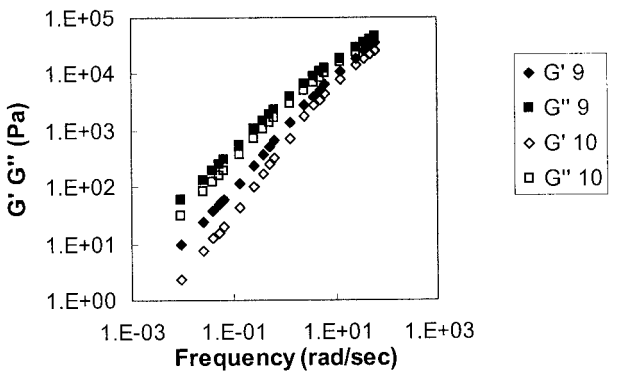

Figure 8 Influence of LCBF on G' and G'' for samples 9 and 10.

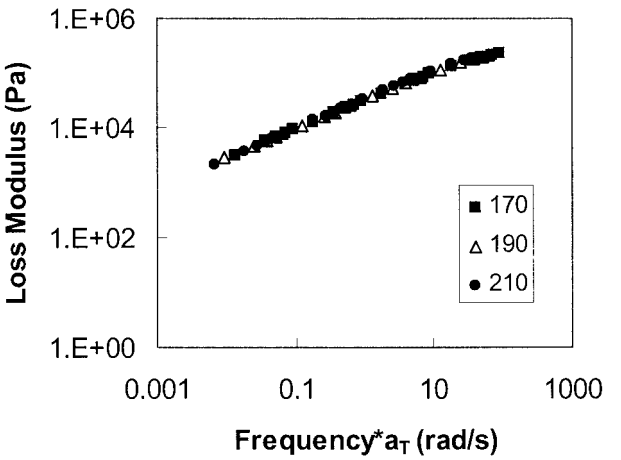

Figure 9 Apparent master curve of sample 7 (E_a = 31.4 kJ/mol).

Sample 9, with an M_w of 63 kmol/g and an LCBF of 0.20, had enhanced values of G' and G'' at low shear rates compared to sample 10, with an M_w of 57 kmol/g and an LCBF of 0.17. At higher shear rates, G' and G'' were similar for both samples. Again, increased levels of LCB led to a broader relaxation spectrum. The G'_0 of these samples could not be determined because the loss modulus plateau was located outside the experimental range. Samples 9 and 10 differed from samples 2 and 8 in that the crossover points G_x, which separated viscouslike and elasticlike behavior, were not apparent under the experimental frequency range.

An attempt was made to superimpose the rheological data, generated at multiple temperatures, to 190°C using the shift factor a_T given in eq. (5):

$$a_T = \exp\left[\frac{E_a}{R}\left(\frac{1}{T} - \frac{1}{T_0}\right)\right] \tag{5}$$

This was only partially successful, however, as the shift factor of several of the LCB PEs showed a dependence on both the temperature and the shear rate. Therefore, the loss modulus, storage modulus, and dynamic viscosity were all given at 190°C. A careful examination of the data was required to determine the rheological complexity. Figure 9 shows an apparent master curve for the loss modulus of sample 7.

A single-frequency shift factor was used at each temperature and the data appeared to superimpose well. However, at low and high frequencies, there was a slight lack of fit in the data. This lack of fit was due to using an average activation energy to determine a_T at all frequencies. A method of detecting the thermorheological complexity is to plot the magnitude of the complex modulus versus the product of η_0 and the frequency. These plots are temperature-independent for simple materials and temperature-dependent for complex materials. Figure 10 shows the simple behavior of sample 10, while Figure 11 shows the complex behavior of sample 7. Each of the samples was analyzed using this method, with the majority of samples showing complex behavior.

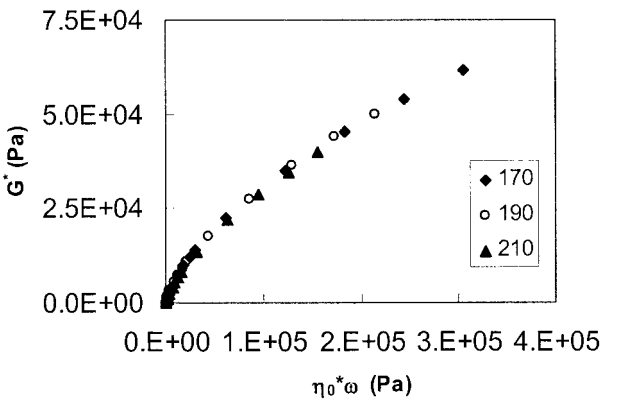

Figure 10 Rheologically simple behavior of sample 10.

The values of a_T at various frequencies were determined using the storage modulus. Plots of G' versus frequency at 170 and 190°C were constructed for each of the samples. A value of G' at 170°C was chosen and the value of the frequency was noted. The frequency at the same value of G' was then determined. The value of a_T was calculated using eq. (6) shown below:

$$a_T(G', 210) = \frac{\omega_{170}}{\omega_{210}} \tag{6}$$

The values of a_T for the remaining values of G' were determined in a similar manner. Figure 12 shows the method of determining a_T used for sample 5. The shift factors for each sample were calculated in an analogous fashion.

The activation energy at various frequencies for the samples was determined using eq. (5). Figure 13 shows the values of E_a for several samples, with the remaining samples excluded to improve clarity. Sam-

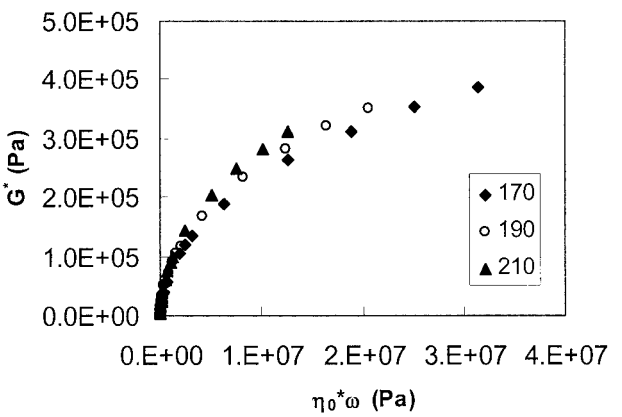

Figure 11 Rheologically complex behavior of sample 7.

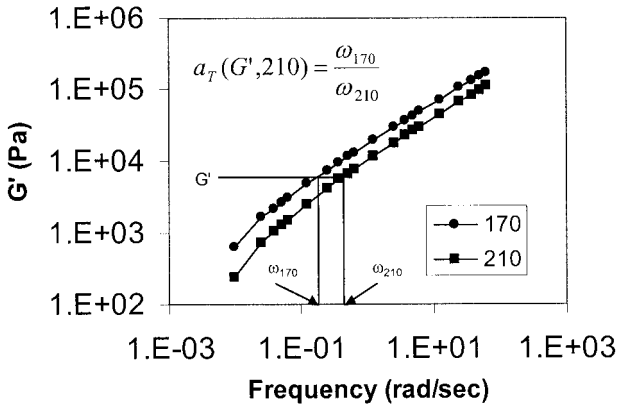

Figure 12 Determination of modulus-dependent shift factor for sample 5.

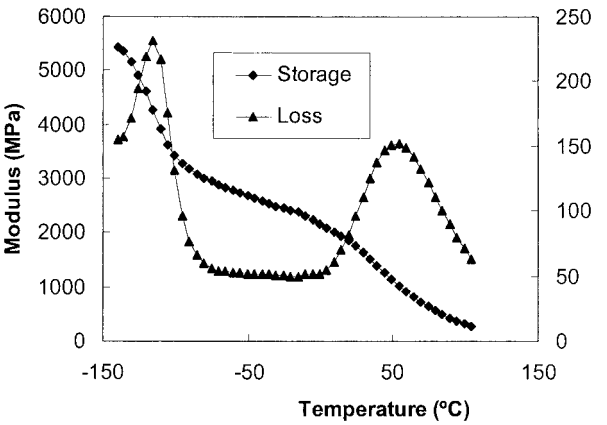

Figure 14 Dynamic mechanical behavior of high-density PE.

ples 5–8 exhibited obvious thermorheological complexity while sample 10 exhibited simple behavior. The activation energy was shear-dependent with the highest values at low shear rates. The E_a value at low shear rates depended on both the LCBF and on the length of the LCB, with values ranging from 39 to 49 kJ/mol. In comparing samples 7 (LCBF = 0.17, M_w = 160 kg/mol) and 8 (LCBF = 0.07, M_w = 152 kg/mol), the former had significantly higher activation energies at low shear rates. This enhancement of E_a was attributed to the increase in LCBF. Meanwhile, sample 7 (LCBF = 0.17, M_w = 160 kg/mol) had a similar LCBF to sample 10 (LCBF = 0.17, M_w = 57 kg/mol) yet exhibited significantly different activation energies.

The E_a of linear polymers, with molecular weights above the critical entanglement length, has been demonstrated to be independent of molecular weight.[19] Therefore, the increase in E_a from sample 10 to sample 7 was attributed to the difference in the LCB length. At higher shear rates, the E_a's of the samples decreased to a similar value of about 32 kJ/mol. This complex behavior was due to multiple relaxation regimes with different temperature sensitivities. The high-frequency activation energies were due primarily to the flow of linear chains. Consequently, despite having different LCBFs and M_w's, the samples all had similar high-frequency E_a's. The low-frequency activation energies were due to the cumulative effect of the relaxations of molecules with various branch structures. LCBs had different relaxation mechanisms with different temperature sensitivities than those of the linear chains. Samples with high LCBFs or with high LCB lengths had elevated values of E_a.

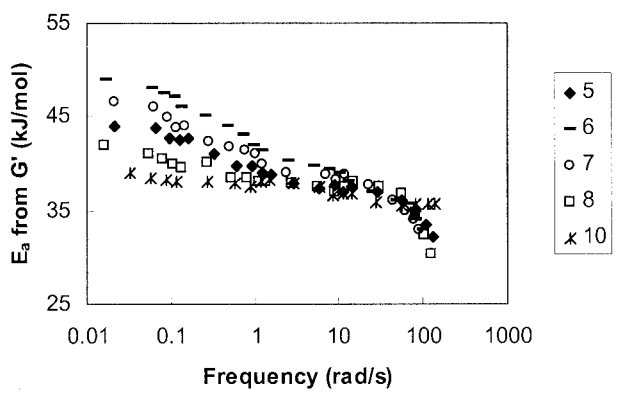

Figure 13 Frequency-dependent activation energy.

Thermomechanical properties

The influence of the LCBF and the polymer M_w on the storage modulus E', loss modulus E'', and γ-, β-, and γ-relaxations at lower temperatures were investigated using a dynamical mechanical analyzer. The data are summarized in Table II. Figure 14 shows the dynamic mechanical behavior of sample 2 (M_w = 154 kg/mol, LCBF = 0.12), which is representative of high-density PE. There were only two thermal relaxations present in the loss modulus curves. The α-relaxation was located at 52.2°C, while the γ-relaxation was found at −115.7°C. None of the LCB PE samples displayed a β-relaxation process. The β-relaxation peak was thought to be due to the motion in the amorphous phase near branch points or to the glass transition of loose loop and intercrystalline tie molecules in ultrahigh molecular weight PE.[20,21] The branch content of these slightly branched samples was too low to exhibit a β-relaxation process.

To determine the influence of LCB on the dynamic mechanical properties of PE, an effort was made to produce samples with varying LCBFs and similar molecular weights. The storage modulus and loss modulus of samples 3 (M_w = 108 kg/mol, LCBF = 0.03), 4 (M_w = 95 kg/mol, LCBF = 0.22), and 5 (M_w = 122 kg/mol, LCBF = 0.21) are shown in Figures 15 and 16. Figures 17 and 18 show those of samples 2 (M_w = 154

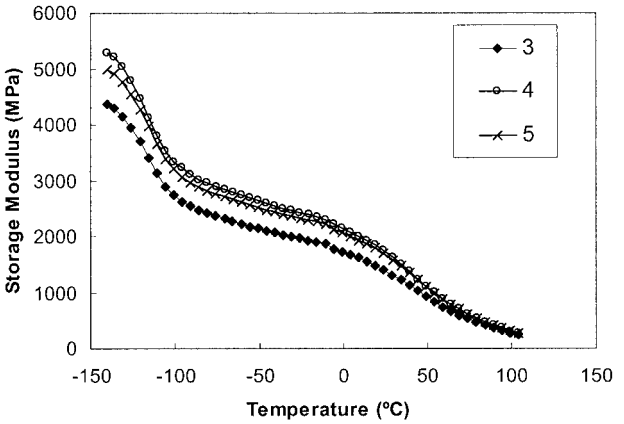

Figure 15 Storage modulus of samples 3, 4, and 5.

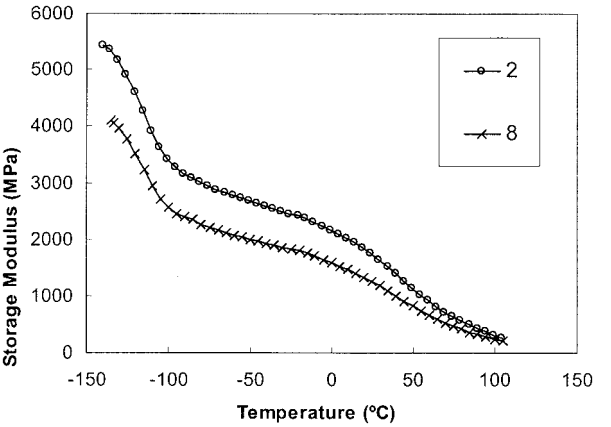

Figure 17 Storage modulus of samples 2 and 8.

kg/mol, LCBF = 0.12) and 8 (M_w = 152 kg/mol, LCBF = 0.07). These samples had similar molecular weights and polydispersity indexes and, therefore, any variation in behavior was attributed to LCB.

The LCBF had a significant influence on the PE storage modulus. The storage modulus of sample 3 (LCBF = 0.03), shown in Figure 15, was significantly lower than that of sample 4 (LCBF = 0.22) at all temperatures below the α-relaxation point. Sample 4, moreover, responded in an almost identical fashion as that of sample 5 (LCBF = 0.21). In a similar manner, sample 8 (LCBF = 0.07) had a significantly lower storage modulus than that of sample 2 (LCBF = 0.12), as seen in Figure 17. In all cases, an increase in the LCBF led to an increase in the storage modulus at all temperatures below the α-relaxation point.

The LCBF also showed a significant influence on the loss modulus, as seen in Figures 16 and 18. In all the measured samples, an increase in the LCBF led to enhanced values of E''. Samples 4 and 5, with similar LCBFs, responded in an almost identical manner while sample 3 had a significantly lower E''. Sample 2 exhibited enhanced values of E'' at all measured temperatures compared to sample 8. The studies showed a correlation with the values of the loss modulus and the impact strength, with elevated values of E'' leading to improvements in impact toughness.[22]

There has been much research conducted on PE and polypropylene treated with peroxides and/or radiation.[23,24] The effects of such treatments are bond scission and the formation of inter- and intramolecular crosslinks. It was demonstrated that the storage modulus of high molecular weight PE increases with increasing radiation dosages.[23] Furthermore, there was little influence on the tan δ response, indicating an increase in the loss modulus. Other authors observed an increase in E' by the addition of low levels of peroxide to PE.[24] With increased peroxide concentration, the E' of PE showed a sharp decline, possibly due to chain scission. The enhancement in the storage modulus was explained by stiffening due to crosslinking in the amorphous phase and to a suppression of c-axis slip in the lamellae by internal or surface crosslinking in the crystal phase. LCB has a similar architecture to crosslinked chains and is therefore ex-

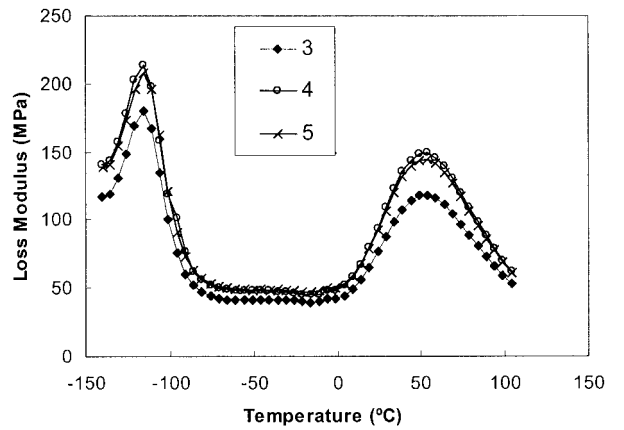

Figure 16 Loss modulus of samples 3, 4, and 5.

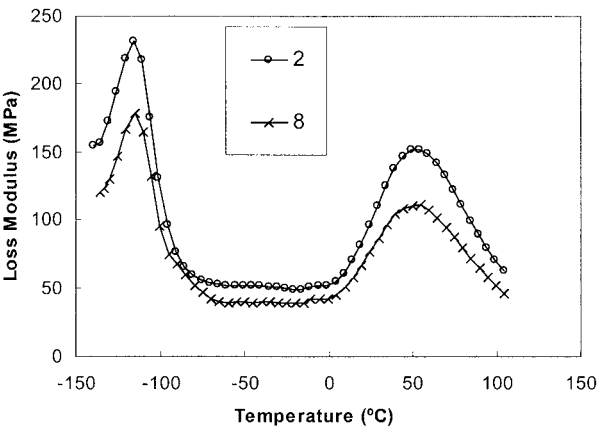

Figure 18 Loss modulus of samples 2 and 8.

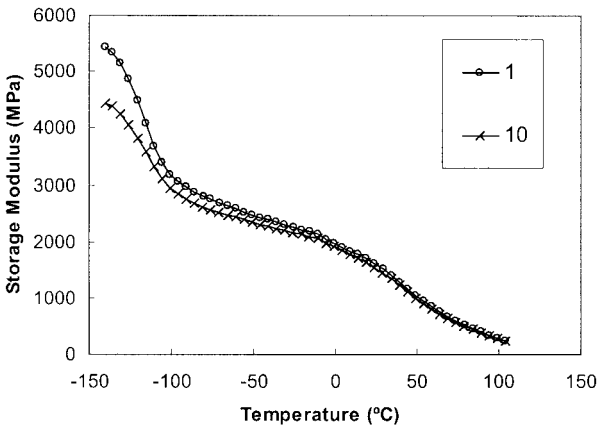

Figure 19 Storage modulus of samples 1 and 10.

pected to behave in a similar manner. Consequently, the enhancements in E' and E'' observed in this work can be attributed to the same mechanisms described for crosslinked PE.

The influence of molecular weight on the storage modulus and loss modulus was also examined. Two PE samples with widely different molecular weights but with similar LCBFs were examined. Figures 19 and 20 show the storage modulus and loss modulus of samples 1 (M_W = 280 kg/mol, LCBF = 0.16) and 10 (M_W = 57 kg/mol, LCBF = 0.17). The molecular weight of the samples had little influence on the dynamic mechanical properties at temperatures above the γ-relaxation point (glass transition temperature). Despite having an M_W almost five times higher, sample 1 behaved in a similar manner to sample 10 except at temperatures below −100°C. This indicates that the molecular weight of the samples did not have a strong influence on the crystallinity.

LCB appeared to have little influence on the thermal relaxations of PE. None of the samples studied exhibited a β-relaxation peak, indicating that the levels of branching were too low to produce sufficient amorphous regions. The LCBF and M_w showed little influence on the γ-relaxation process with values in the range of −115.41 to −117.15°C.

The γ-relaxation is generally believed to be due to crankshaft rotation of short methylene main-chain segments at the surface of polymer crystals. The peak shifts to lower temperatures and sharpens with decreasing short-chain branch content. However, LCB at low levels did not appear to alter the crystallinity of the polymer enough to influence the γ-relaxation process. The α-relaxation process also appeared to be unaffected by the M_w and LCBF of the polymer. This process, thought to be due to motion within the crystalline phase, intensifies with increasing crystallinity.[25] The α-relaxation is influenced by the crystallite thickness and crystal imperfections but is thought to be independent of branch type and molecular weight. It was demonstrated that low levels of LCB did not have sufficient influence on the crystallinity of PE to affect the α-relaxation process.

CONCLUSIONS

The rheological properties of long-chain-branched PEs were shown to be significantly different from their linear analogs. The samples had higher η_0's and exhibited greater shear thinning than those of linear PEs with similar molecular weights. These enhancements were attributed to the formation of additional entanglements between polymer molecules, leading to increased resistance to flow. At higher shear rates, these entanglements broke, allowing normal viscosities. Consequently, elevated LCBFs led to higher η_0's and greater shear thinning. LCB also influenced the loss modulus and storage modulus. Elevated LCBFs led to enhanced values of G' and G'' at low shear rates, yet had little influence at higher shear rates. Long-chain-branched PEs also exhibited broader relaxation spectrums than those of linear PEs. The samples exhibited thermorheologically complex behavior. The temperature sensitivity could not be summarized with a single shift factor. The activation energy, which was shear-dependent, was determined using G'. Higher LCBFs and LCB lengths led to elevated values of E_a at low shear rates. At high shear rates, the values of E_a were equivalent to those of linear polymers.

LCB also played a significant role in the dynamic mechanical behavior. Increasing the frequency of branching increased the stiffness of the polymer, as reflected by the storage modulus. LCB also served to enhance the damping or energy dissipation of PE, shown by increased values of the loss modulus. These PEs showed behavior similar to PE crosslinked by radiation or peroxide and a similar mechanism was used to explain the dynamic mechanical differences. The enhancements in E' were attributed to stiffening

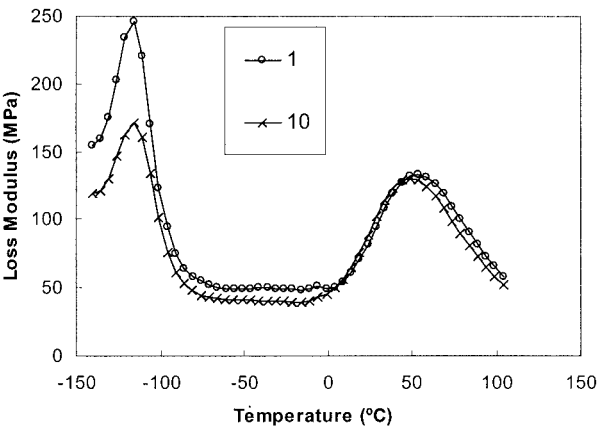

Figure 20 Loss modulus of samples 1 and 10.

due to crosslinking in the amorphous phase and to a suppression of *c*-axis slip in the lamellae by internal or surface crosslinking in the crystal phase. The long-chain-branched PEs produced in this work had several notable benefits over crosslinked PE. LCB had little influence on the crystalline structure of the PE. The α- and γ-relaxations showed little dependence on the LCBF.

The authors wish to thank the Ministry of Education, Science and Technology of Ontario (MEST) for the PREA support for the work. We would also like to thank the Canada Foundation of Innovation (CFI) for the support for the research facilities.

References

1. Vega, J. F.; Munoz-Escalona, A.; Santamaria, A.; Munoz, M. E.; Lafuente, P. Macromolecules 1996, 29, 960.
2. Bersted, B. H.; Slee, J. D.; Richter, C. A. J Appl Polym Sci 1981, 26, 1001; Bersted, B. H. J. Appl Polym Sci 1985, 30, 3751.
3. Tsenoglou, C. J.; Gotsis, A. D. Macromolecules 2001, 34, 4685.
4. Carella, J. M.; Gotro, J. T.; Graessley, W. W. Macromolecules 1986, 19, 659.
5. Kokko, E.; Malmberg, A.; Lehmus, P.; Lofgren, B.; Seppala J. V. J Polym Sci Polym Chem 2000, 38, 376.
6. Beigzadeh, D.; Soares, J. B. P.; Duever, T. A. Macromol Symp 2001, 173, 179.
7. Doerpinghaus, P. J.; Baird, D. G. Macromolecules 2002, 35, 10087.
8. Shroff, N.; Mavridis, H. Macromolecules 1999, 32, 8454; Shroff, N.; Mavridis, H. Macromolecules 2001, 34, 7362.
9. Small, P. A. Adv Polym Sci 1975, 18, 1.
10. Santamaria, A. Mater Chem Phys 1985 12, 1.
11. Jordan, E. A.; Donald, A. M.; Fetters, L. J.; Klein, J. ACS Polym Prepr 1989, 30, 63.
12. Yan, D.; Wang, W.-J.; Zhu, S. Polymer 1999, 40, 1737.
13. Kaminsky, W. In Transition Metal Catalyzed Polymerization; Quirk, R. P., Ed.; MMI: London, 1983; Vol. 4, p 225.
14. Chien, J. C. W.; Wang, B. P. J Polym Sci Polym Chem Ed 1988, 26, 3089.
15. Wang, W.-J.; Yan, D.; Zhu, S.; Hamielec, A. E. Macromolecules 1998, 31, 8677; Wang, W.-J.; Yan, D.; Charpentier P. A.; Zhu, S.; Hamielec, A. E.; Sayer, B. Macromol Chem Phys 1998, 199, 2409.
16. Lai, S. Y.; Wilson J. R.; Knight, G. W.; Stevens, J. C.; Chum, P. W. S. U.S. Patent 5 272 236, 1993 (to Dow Chemical Co.).
17. Kolodka, E.; Wang, W.-J.; Charpentier, P. A.; Zhu, S.; Hamielec, A. E. Polymer 2000, 41, 3985.
18. Cross, M. M. J Colloid Sci 1965, 20, 417.
19. Wood-Adams, P.; Dealy, J. M. Macromolecules 2000, 33, 7489; Wood-Adams, P.; Costeux, S. Macromolecules 2001, 34, 6291.
20. Ohta, Y.; Yasuda, H. J Polym Sci Polym Phys 1994, 32, 2241.
21. Stark, P.; Malmberg, A.; Lofgre, B. J Appl Polym Sci 2002, 83, 1140.
22. Jafari, S. H.; Gupta, A. K. J Appl Polym Sci 2000, 78, 962.
23. Birkinshaw, C.; Buggy, M.; White J. J. Mater Chem Phys 1986, 14, 549.
24. Kuenert, K. A. J Macromol Sci-Chem 1982, 17, 1469.
25. Nitta, K.-H.; Tanaka, A. Polymer 2001, 42, 1219.